AIAA JOURNAL
Vol. 31, No. 1, January 1993

Numerical Simulation of Viscous Liquid Sloshing in Arbitrarily Shaped Reservoirs

G. Popov,* G. H. Vatistas,† S. Sankar,‡ and T. S. Sankar‡
Concordia University, Montreal, Quebec, Canada

Abstract

A NOVEL approach for the application of the reflection-type boundary conditions for a liquid with an interface in arbitrarily shaped containers, subjected to a step frame acceleration, is presented. The two-dimensional sloshing problem is solved numerically using a modified marker and cell method that has been altered to accommodate the new boundary conditions. Application of the method to predict the dynamic behavior of liquids in rectangular and cylindrical containers is also included.

Contents

The prediction of dynamic loading arising from liquid sloshing is crucial in many engineering applications. The linear theories of liquid sloshing[1-4] currently in use give sufficiently accurate solutions for small amplitudes of liquid oscillations. However, in the majority of real situations these solutions become inaccurate. In this case a numerical solution based on the Navier-Stokes, continuity, and free-surface equations with correctly imposed boundary conditions is appropriate.

The correct application of boundary conditions for the free-surface flow problem is a difficult task. Often the conventional reflection, Abbett's,[5] Viecelli's,[6] and Nichols and Hirt's[7] methods are used. The reflection method is the simplest, but it is not accurate on boundaries with high curvature. Abbett's and Viecelli's methods are more accurate, but are very complicated. Furthermore, these methods are applied to boundary points lying exactly on the boundary (i.e., an irregular mesh has to be used). The proposed method, which we call the "interpolation-reflection method," combines simplicity and adequate accuracy and gives the boundary values directly on the boundary points of a regular staggered grid for arbitrarily shape boundaries. A brief description is presented in this paper. For more extensive treatment the reader should consult the accompanying paper. If the boundary grid point is lying inside the flow domain, the boundary value is computed by interpolation (in the direction normal to the boundary) of an appropriate order (i.e., first or second). If the point is located outside the flow (a fictitious grid point), then the boundary value is also interpolated on the point that is a mirror reflection of the boundary point with respect to the wall. Following this, the computed value is reflected to the boundary point using odd or even symmetry for the no-slip or free-slip condition, respectively.

The derivation of the boundary V velocity for the free-slip condition and second-order interpolation is illustrated in Fig. 1. One can see that the line traced normal to the wall from the boundary point B to the center of the wall curvature O intersects the grid lines in nodes 1 and 2. The location of these nodes depends on the angle α. For second-order interpolation there are four possible configurations described in the accompanying paper. The nodal velocities V_1 and V_2 (previously interpolated between points 3 and 6 and 6 and 7, respectively) are resolved into a normal and tangential components with respect to the local n-τ coordinates. Then the boundary velocity is computed by interpolation between V_1 and V_2 for point B′ and it stands as it is, or it is further reflected to B, depending whether B′ or B is the boundary point of interest.

The normal and tangential components of nodal velocities are

$$V_{n1} = V_1 \sin\alpha, \qquad V_{n2} = V_2 \sin\alpha$$
$$V_{\tau 1} = V_1 \cos\alpha, \qquad V_{\tau 2} = V_2 \cos\alpha \tag{1}$$

The factor m and the interpolation lengths, lying on the n axis, are defined as follows:

$$m = \frac{\delta Y}{\delta X \tan\alpha}; \qquad a = -\frac{l}{\cos\alpha}; \qquad b = \frac{\delta X + l}{\cos\alpha}$$
$$c = \frac{\delta Y}{\sin\alpha} - \frac{\delta X}{\cos\alpha}; \quad l = R\cos\alpha - A \tag{2}$$

Applying Newton's interpolation for unequally distributed nodes and performing the reflection of the V velocity components to point B as $V_{\tau b} = V'_{\tau b}$ and $V_{nb} = -V'_{nb}$, we obtain

$$V_{nb} = (\sum \eta_{in} V_i)\sin\alpha; \qquad V_{\tau b} = (\sum \eta_{i\tau} V_i)\cos\alpha \tag{3}$$

where the weighting coefficients η_i, accounting for the local velocities contribution, are listed in the accompanying paper. Furthermore, the boundary velocity V_b, seen as the projection of the total velocity vector V_{bt} on the Y axis, can be found using the following expressions:

$$V_b = V_{bt}\cos\alpha; \quad V_{bt} = \sqrt{V_{nb}^2 + V_{\tau b}^2}; \quad \beta = (\pi/2) + \alpha - \gamma \tag{4}$$

which together with Eq. (3) give

$$V_b = (\sum \eta_{i\tau} V_i)\cos^2\alpha - (\sum \eta_{in} V_i)\sin^2\alpha; \quad \alpha = \arctan B/A \tag{5}$$

For the U boundary velocity, the formula (5) is slightly changed, i.e.,

$$U_b = (\sum \eta_{i\tau} V_i)\sin^2\alpha - (\sum \eta_{in} V_i)\cos^2\alpha \tag{6}$$

Thus, Eqs. (5) and (6) give explicitly the boundary velocities on the fictitious grid points for free-slip condition and second-order interpolation. If the boundary points are lying inside the flow, then no reflection is required, and the weighting coefficients for the tangential velocity are to be used for calculations of boundary velocities, i.e.,

$$V_b = \sum \eta_{i\tau} V_i; \qquad U_b = \sum \eta_{i\tau} U_i \tag{7}$$

Consider now the no-slip boundary condition. It is easy to show that, in the case of fictitious grid points, the angle β between the total vector velocity V_{bt} and the Y axis equals zero (i.e., $V_b = V_{bt}$). Therefore,

$$V_b = \sum \eta_{in} V_i; \qquad U_b = \sum \eta_{in} U_i \tag{8}$$

Received March 9, 1991; synoptic received May 5, 1992; accepted for publication June 24, 1992. Full paper available from AIAA Library, 555 West 57th Street, New York, NY 10019.

*Research Associate, Department of Mechanical Engineering.
†Associate Professor, Department of Mechanical Engineering. Member AIAA.
‡Professor, Department of Mechanical Engineering.

For points located inside the flow, expressions (7) have to be used. Equations (5–8) stand for any order of interpolation; however, the weighting coefficients have to be changed. For the first order the coefficients are given in the accompanying paper.

At the free surface, the free-slip condition for both the normal and the tangential velocity components must be applied [i.e., Eqs. (7)]. Angle α, which in this case represents the positive and negative slopes of the free surface, is redefined as

$$\alpha = \arctan \frac{\delta X}{H_{i-1} - H_i}; \qquad \alpha = \arctan \frac{\delta X}{H_{i+1} - H_i} \tag{9}$$

where i is referred to the liquid height at the boundary point. Note that the free surface is approximated by a straight line between each pair of the mesh columns.

A series of numerical and physical (in the rectangular Plexiglas tank of size $0.8 \times 0.3 \times 0.57$ m) experiments were carried out to validate the novel boundary conditions formulation. The main conclusions of this experimentation are briefly summarized in the following:

1) The best results are obtained using second-order interpolated-reflected boundary values with no-slip condition at the rigid boundary and free-slip condition at the free boundary.

2) The free-slip and no-slip conditions are more appropriate for Reynolds numbers (Re) $\geq 10^5$. For smaller Re the no-slip condition formulation is more accurate.

3) The second-order interpolation is generally more accurate by comparison than the first order. However, in the regions between the wall and free surface, where the liquid forms sharp edges (typically resolved by one cell), the second-order formulation may fail. In this case grid refinement is recommended.

The previously described boundary conditions formulation was applied to the sloshing problem in rectangular and cylindrical circular containers subjected to a step input horizontal acceleration. The numerical solutions have been obtained in terms of amplitudes and frequencies of the main parameters, such as heights of the free surface, forces, and overturning moments on the container. The natural damped frequencies were normalized as

$$K = \Omega / \sqrt{g(1 + G_x^2)^{1/2}/L_0} \tag{10}$$

where $G_x = g_x/g$ is the dimensionless horizontal acceleration, Ω is the circular frequency, and L_0 is the characteristic length (diameter for a circular container). The marker and cell method developed by Hirt et al.[8] was modified to accommodate the new boundary condition and to maintain the conservation of the liquid mass. In fact, the first-order interpolation-reflection no-slip boundary conditions were applied at the rigid wall and zero order free-slip condition at the free surface. For rectangular containers an 18×10 grid, full upstream differencing, and 0.02-s time increments were employed. Computational stability was ensured by the proper choice of the time and space increments, as suggested in Ref. 8.

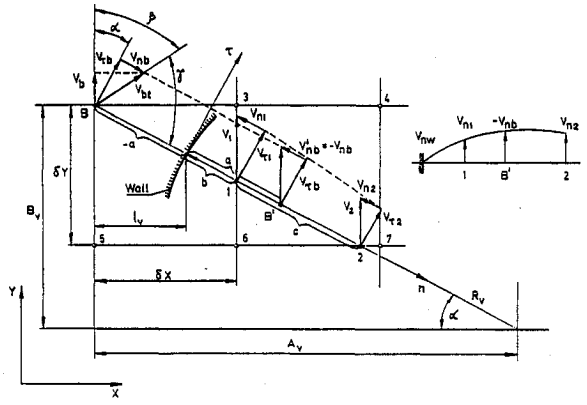

Fig. 1 Derivation of the V boundary velocity for the free-slip condition.

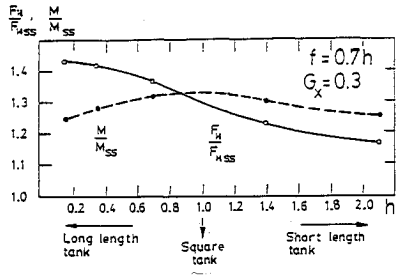

Fig. 2 Dynamic coefficients of the force and moment as functions of the container height.

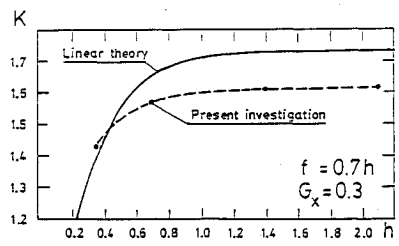

Fig. 3 Normalized damped natural frequency of fluid oscillation in rectangular containers.

Sample results (full parametric studies can be found in Ref. 9) for rectangular containers are shown in Figs. 2 and 3. The dynamic coefficients of the horizontal force and moment, representing the ratios of the dynamic peak values to the corresponding steady-state values, are plotted against the nondimensional container height h for a fixed fill level $f = 0.7$, and $G_x = 0.3$. It is seen that the most intense sloshing, with respect to the overturning moment, occurs in a square container, $h = 1$, whereas the peak of the dynamic coefficient of the force falls to small values of the container height. The computed first mode damped frequency (see Fig. 3) is 5–7% lower than the frequency given by the linear theory, except for containers of low height, where the first mode vibration is strongly affected by the action of the horizontal top wall of the tank.

References

[1]Moiseyev, N. N., "On the Theory of Nonlinear Vibration of a Liquid of Finite Volume," *Applied Mathematics and Mechanics (PMM),* Vol. 22, No. 5, 1958, pp. 860–870.

[2]Abramson, H. N., "The Dynamic Behavior of Liquids in Moving Containers," NASA SP-106, 1966.

[3]Faltinsen, O. M., "A Nonlinear Theory of Sloshing in Rectangular Tanks," *Journal of Ship Research,* Vol. 18, No. 4, 1974, pp. 224–241.

[4]Bauer, H. F., "Dynamic Behavior of an Elastic Separating Wall in Vehicle Containers," Part 1, *International Journal of Vehicle Design,* Vol. 2, No. 1, 1981, pp. 44–77.

[5]Abbett, M. J., "Boundary Condition Calculation Procedures for Inviscid Supersonic Flow Field," *Proceedings of the AIAA Computational Fluid Dynamics Conference,* Palm Springs, CA, 1973, pp. 153–172.

[6]Viecelli, T. A., "A Method for Including Arbitrary External Boundaries in the MAC Incompressible Fluid Computing Technique," *Journal of Computational Physics,* Vol. 4, 1969, pp. 543–551.

[7]Nichols, B. D., and Hirt, C. W., "Improved Free Surface Boundary Conditions for Numerical Incompressible Flow Calculations," *Journal of Computational Physics,* Vol. 8, No. 3, 1971, pp. 434–338.

[8]Hirt, C. W., Nichols, B. D., and Romero, N. C., "SOLA—A Numerical Solution Algorithm for Transient Fluid Flow," Los Alamos Sci. Lab. Rept. LA-5852, 1975.

[9]Popov, *G.*, "Dynamics of Liquid Sloshing in Road Containers," Ph.D. Dissertation, Dept. of Mechanical Engineering, Concordia University, Montreal, Canada, 1991.

[10]Budiansky, B., "Sloshing of Liquids in Circular Canals and Spherical Tanks," *Journal of the Aero/Space Sciences,* Vol. 27, No. 3, 1960, pp. 161–173.